Supporting Information for "Experimental and model-based scalability assessment of pH-shift electrolyzers for neutral salt reduction"

Jonas Görtz[1], Stine Kuhlemann[1], Yusuf Alperen Değirmenci[1], Jan Haß[1], Andreas Jupke[1,2*]

[1]Fluid Process Engineering (AVT.FVT), RWTH Aachen University, Forckenbeckstrasse 51, Aachen, 52074, North-Rhine Westphalia, Germany.
[2]Institute for Bio- and Geosciences (IBG-2), Forschungszentrum Jülich GmbH, Wilhelm-Johnen-Straße, Jülich, 52428, North-Rhine Westphalia, Germany.

*Corresponding author(s). E-mail(s): andreas.jupke@avt.rwth-aachen.de;
Contributing authors: jonas.goertz@avt.rwth-aachen.de;
stine.kuhlemann@avt.rwth-aachen.de; yusuf.degirmenci@rwth-aachen.de;
jan.hass@avt.rwth-aachen.de;

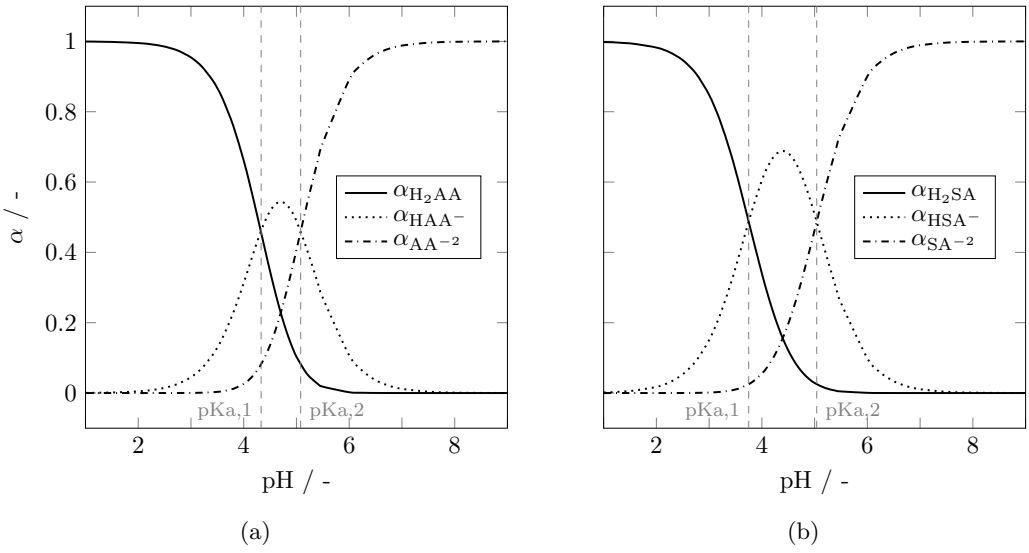
S.1 Properties of adipic and succinic acid

S.1.1 Dissociation reaction

Table S.1 lists the implemented forward and backward reactions in the numerical framework to calculate the concentration fields within the electrolyzers. Further, the assumed and measured pK_a values for adipic acid are also included. Fig. S.1 depicts the dissociation of adipic and succinic acid. α_0, α_1, and α_2 represent the molar fraction of the fully protonated, mono-dissociated and fully dissociated acid species, respectively. The pK_a value are given in Tab. S.1.

Table S.1: Acid–base reactions implemented in the numerical simulations, with forward/backward Arrhenius parameters ($k = A T^{\beta} \exp(-T_a/T)$).

System	Reaction	Dir.	A	β	T_a [K]	pK_a
Water auto-ionisation	$H_2O \rightarrow H^+ + OH^-$	fwd	2.5298×10^{-5}	0	0	–
	$H^+ + OH^- \rightarrow H_2O$	rev	1.4×10^{11}	0	0	–
Succinic acid, 1st diss.	$H_2SA \rightarrow H^+ + HSA^-$	fwd	1×10^2	0	0	4.21
	$H^+ + HSA^- \rightarrow H_2SA$	rev	2.138×10^6	0	0	–
Succinic acid, 2nd diss.[a]	$HSA^- \rightarrow H^+ + SA^{2-}$	fwd	1×10^2	0	0	5.64
	$H^+ + SA^{2-} \rightarrow HSA^-$	rev	1.202×10^7	0	0	–
Sulfuric acid, 2nd diss.	$HSO_4^- \rightarrow H^+ + SO_4^{2-}$	fwd	1.00×10^2	0	0	1.99
	$H^+ + SO_4^{2-} \rightarrow HSO_4^-$	rev	9.772×10^3	0	0	–



(a) (b)

Fig. S.1: Dissociation of (a) adipc and (b) succinic acid.

S.1.2 Diffusion coefficients

Table S.2 lists the used diffusion coefficients of all involved species (H_2AA, HAA^-, HAA^{2-}, H^+, SO_4^{2-}, and HSO_4^-). Diffusion coefficients for adipic acid were approximated by diffusion coefficients for succinic acid.

Table S.2: Diffusion coefficients at infinite dilution and 25 °C used in the model.

Species	D / $m^2\,s^{-1}$	Source
H^+	9.3×10^{-9}	[1]
OH^-	5.3×10^{-9}	[1]
H_2O	2.3×10^{-9}	[2][a]
AA^{2-}	7.83×10^{-10}	[1]
H_2AA	9.3×10^{-10}	[3–5][b]
HAA^-	8.5×10^{-10}	estimated[c]

[a] Self-diffusion coefficient of water.
[b] Literature values differ: $9.4 \cdot 10^{-10}\,m^2\,s^{-1}$ [3], taken from [4], and $8.8 \cdot 10^{-10}\,m^2\,s^{-1}$ measured at $0.025\,mol\,L^{-1}$ [5]. An intermediate value was used.
[c] No tabulated value available; midpoint of H_2AA and AA^{2-}, assuming a linear relation.

S.2 Definition of protonation efficiency

Using the pH at the start and end of each experiment, $\Delta n_{H^+,acid}$, $\Delta n_{H^+,SO_4}$, and $\Delta n_{H^+,aq}$ are defined for $j \in AA, SA$ by

$$\Delta n_{H^+,acid} = V c_{j,start} \left[2\left(\alpha_{0,j}(pH_{end}) - \alpha_{0,j}(pH_{start})\right) + \alpha_{1,j}(pH_{end}) - \alpha_{1,j}(pH_{start})\right] + n_{j,s}\,, \quad (1)$$

$$\Delta n_{H^+,SO_4} = \left[2\left(\alpha_{0,SO_4}(pH_{end}) - \alpha_{0,SO_4}(pH_{start})\right) + \alpha_{1,SO_4}(pH_{end}) - \alpha_{1,SO_4}(pH_{start})\right]\,, \text{ and} \quad (2)$$

$$\Delta n_{H^+,aq} = V\left(10^{-pH_{end}} - 10^{-pH_{start}}\right)\,, \quad (3)$$

calculated and inserted into equation (3).

S.3 Assembly of 13.7 cm^2 electrolyzer

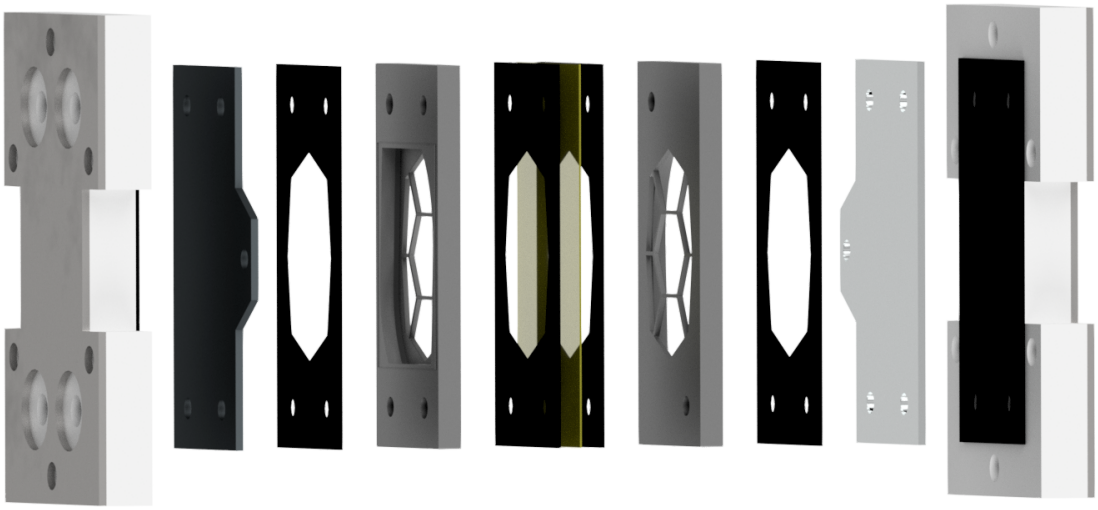


Fig. S.2: Exploded view of the 13.7 cm^2 electrolyzer.

S.4 Further experimental results

Fig. S.3 depicts the course of pH, cell potential, and AA concentration for experiments in the small-sized and medium-sized electrolyzer at an elevated temperature of T=60 °C and i=0.1 A cm^{-2}. Fig. S.4 shows the same experimental results for the SA electrolyte systems at T=60 °C and i=0.1 A cm^{-2}.

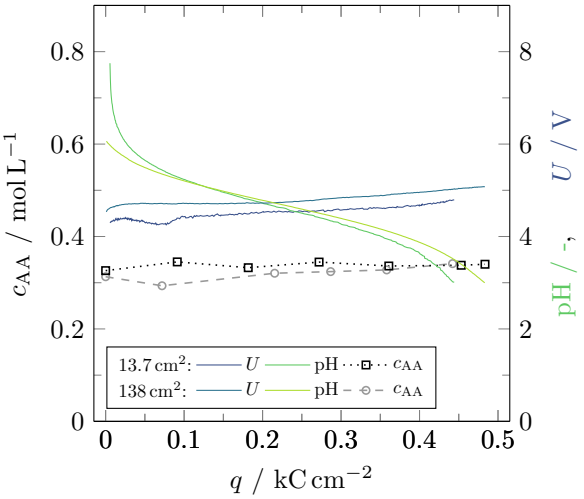


Fig. S.3: Experimental results for i=0.1 A cm^{-2}, T=60 °C, and $c_{AA,0}$=0.34 mol L^{-1} and either A_E=138 cm^2 and $\dot{V}_{el}$=1.5 L min^{-1} or A_E=13.7 cm^2 and $\dot{V}_{el}$=0.15 L min^{-1}.

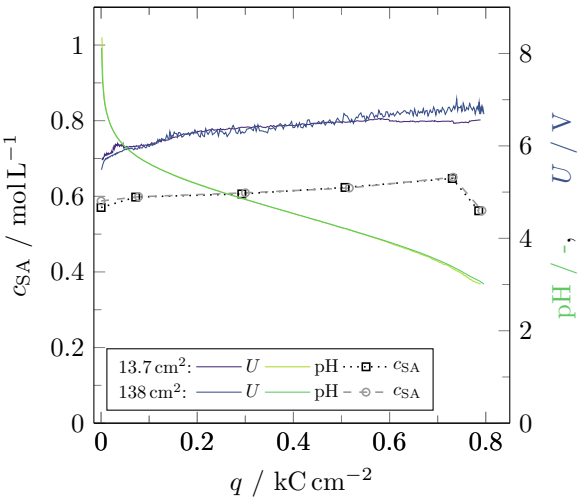


Fig. S.4: Experimental results for i=0.1 A cm^{-2}, T=20 °C, and $c_{SA,0}$=0.62 mol L^{-1} and either A_E=138 cm^2 and $\dot{V}_{el}$=1.5 L min^{-1} or A_E=13.7 cm^2 and $\dot{V}_{el}$=0.15 L min^{-1}.

S.5 Boundary conditions

Table S.3 lists the employed boundary conditions for the simulation of the small-sized and medium-sized electrolyzers.

Table S.3: Boundary conditions applied to each patch of the computational domain.

Patch	**U (velocity)**	p **(pressure)**	k	ω	ν_t
		Small-sized electrolyzer ($A_{\mathbf{E}} = 13.7\,\mathrm{cm}^2$)			
Inlet	`interstitialInletVelocity` $(0,\ 0,\ 0.1136)\ \mathrm{m\,s^{-1}}$	`fixedFluxPressure`	`fixedValue` $8.36 \times 10^{-5}\ \mathrm{m^2\,s^{-2}}$	`fixedValue` $166\ \mathrm{s^{-1}}$	`calculated` $0\ \mathrm{m^2\,s^{-1}}$
Outlet	`pressureInletOutletVelocity`	`fixedValue` 0	`inletOutlet`	`inletOutlet`	`calculated` $0\ \mathrm{m^2\,s^{-1}}$
Walls & Electrode	`noSlip`	`fixedFluxPressure`	`fixedValue` $1 \times 10^{-12}\ \mathrm{m^2\,s^{-2}}$	`zeroGradient`	`zeroGradient`
		Medium-sized electrolyzer ($A_{\mathbf{E}} = 138\,\mathrm{cm}^2$)			
Inlet	`interstitialInletVelocity` $(0,\ 0,\ -6.51 \times 10^{-2})\ \mathrm{m\,s^{-1}}$	`fixedFluxPressure`	`fixedValue` $1.59 \times 10^{-5}\ \mathrm{m^2\,s^{-2}}$	`fixedValue` $28.8\ \mathrm{s^{-1}}$	`calculated` $5.53 \times 10^{-7}\ \mathrm{m^2\,s^{-1}}$
Outlet	`pressureInletOutletVelocity`	`fixedValue` 0	`inletOutlet`	`inletOutlet`	`calculated` $5.53 \times 10^{-7}\ \mathrm{m^2\,s^{-1}}$
Walls & Electrode	`noSlip`	`fixedFluxPressure`	`fixedValue` $1 \times 10^{-12}\ \mathrm{m^2\,s^{-2}}$	`zeroGradient`	`zeroGradient`

Patch	**H**	**H_2O**	**H_2AA**	**HAA**	**HSO_4**	**OH**	**AA**	**SO_4**
Inlet	`fixedValue` in $\mathrm{mol\,m^{-3}}$							
	4.16869×10^{-8}	0.9143984	1.68707×10^{-2}	1.84109×10^{-2}	1.95314×10^{-4}	2.39883×10^{-13}	3.57344×10^{-3}	4.65512×10^{-2}
Outlet	`inletOutlet`							
Walls & Electrode	`zeroGradient`							

S.6 Further simulation results

To ensure a quasi-steady state of the numerical model, the number of bubbles and the velocity weighted pH value at the outlet are plotted against the simulated time in Fig. S.5 and Fig. S.6, respectively. After a simulated time of 10 s the simulations reach steady state. Hence, a simulation time of 25 s is sufficient. Fig. S.8 illustrates the time and z-averaged gas-liquid flow field and velocity magnitude in the small and medium-sized electrolyzer for the four studied current densities (i=0.05–0.2 A cm^{-2}). Fig. S.9 displays the local supersaturation for the four studied current densities within a distance of 3 mm distance to the electrode for both electrolyzer scales. The course follows the pH profile discussed in section 3.3 and Fig. 11.

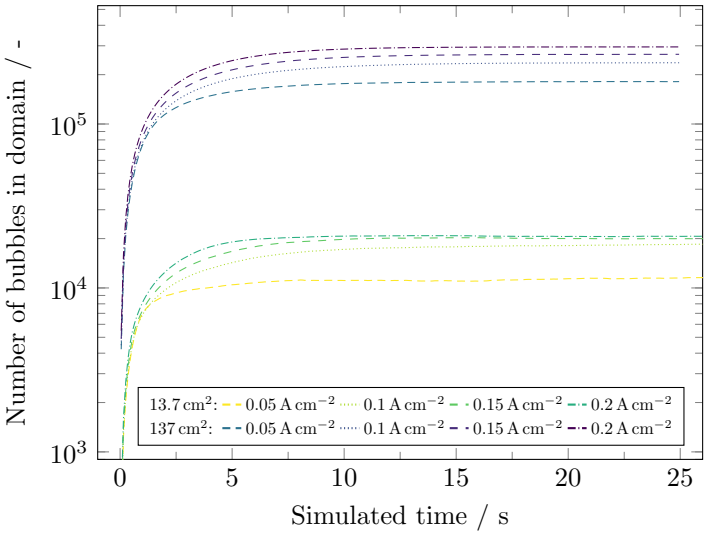


Fig. S.5: Number of Lagrangian parcels (bubbles) against simulation time inside the small-sized and medium-sized electrolyzer domain

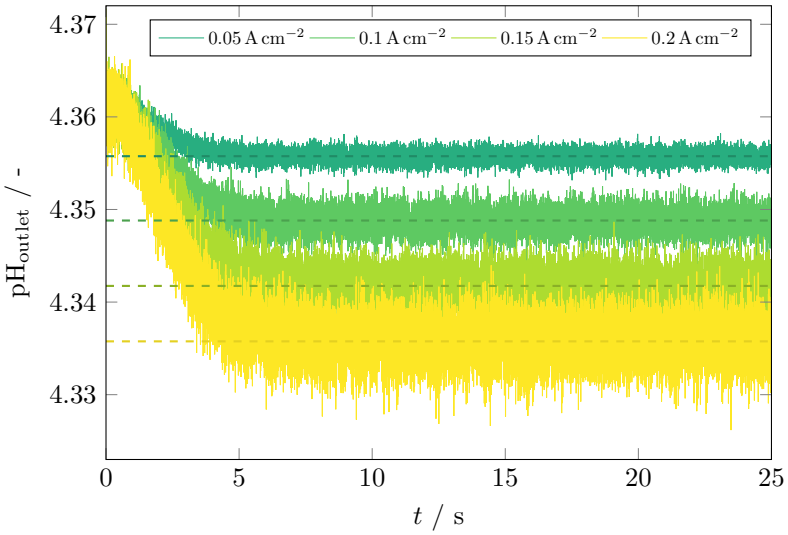
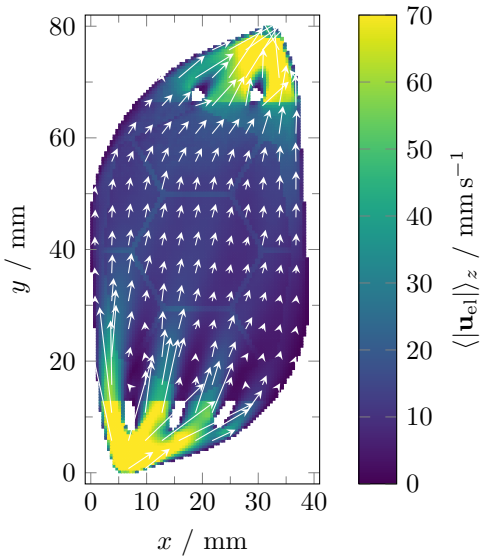
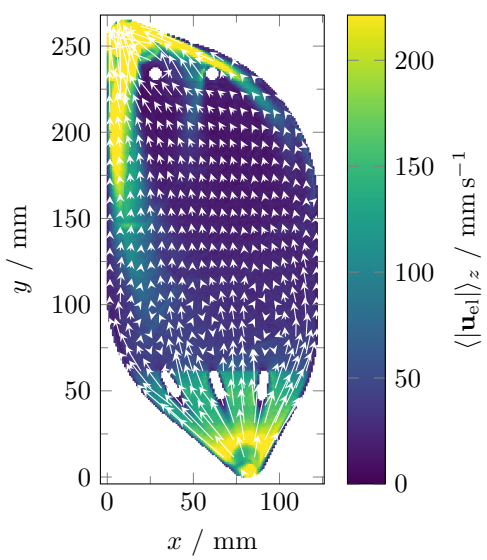


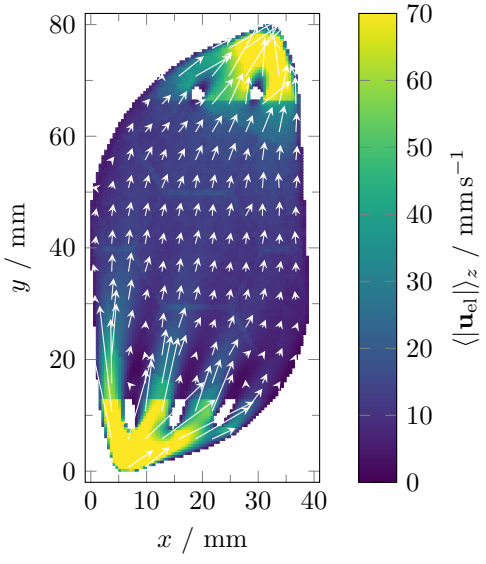
Fig. S.6: Velocity-weighted pH value of the outlet stream for A_E=13.7 cm^2 and i=0.05–0.2 A cm^{-2}.


y / mm
x / mm
⟨|u_el|⟩_z / mm s^−1

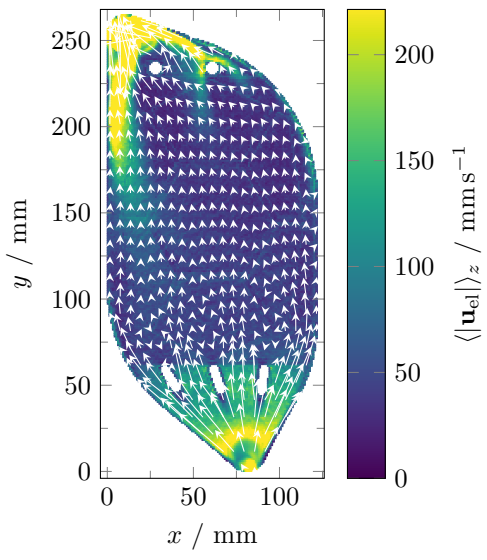
(a)


y / mm
x / mm
⟨|u_el|⟩_z / mm s^−1

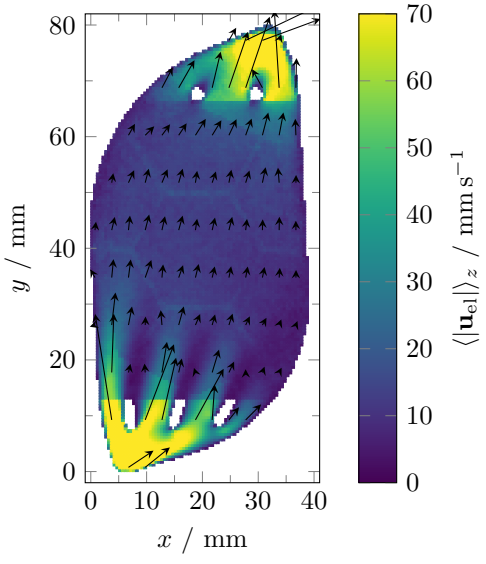
(b)


y / mm
x / mm
⟨|u_el|⟩_z / mm s^−1

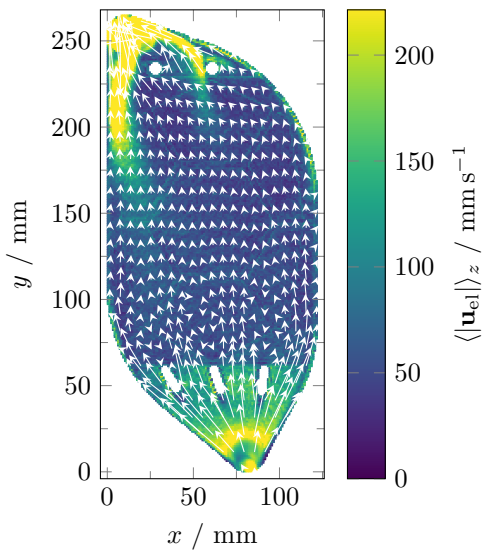
(c)


y / mm
x / mm
⟨|u_el|⟩_z / mm s^−1

(d)


y / mm
x / mm
⟨|u_el|⟩_z / mm s^−1

(e)


y / mm
x / mm
⟨|u_el|⟩_z / mm s^−1

(f)

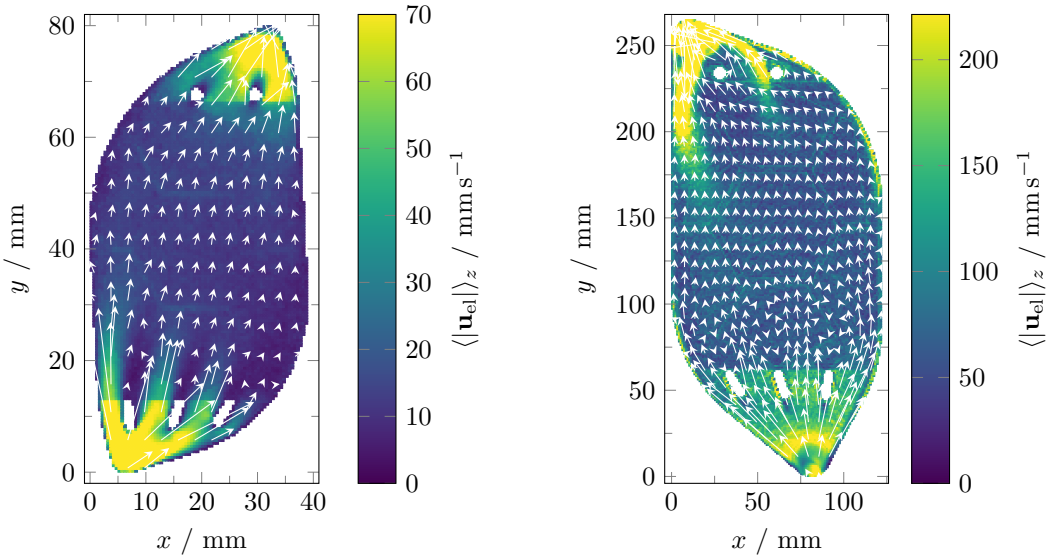


Fig. S.8: Simulated time and z-averaged gas-liquid flow field and velocity magnitude in the (a,c,e,g) 13.6 cm^2 and (b,d,f,h) 136 cm^2 electrolyzer at (a-b) i=0.05 A cm^{-2}, (c-d) i=0.1 A cm^{-2}, (e-f) i=0.15 A cm^{-2}, and (g-h) i=0.2 A cm^{-2}. For better comparison, the velocity magnitude is normalized by the square root of the scaling factor.

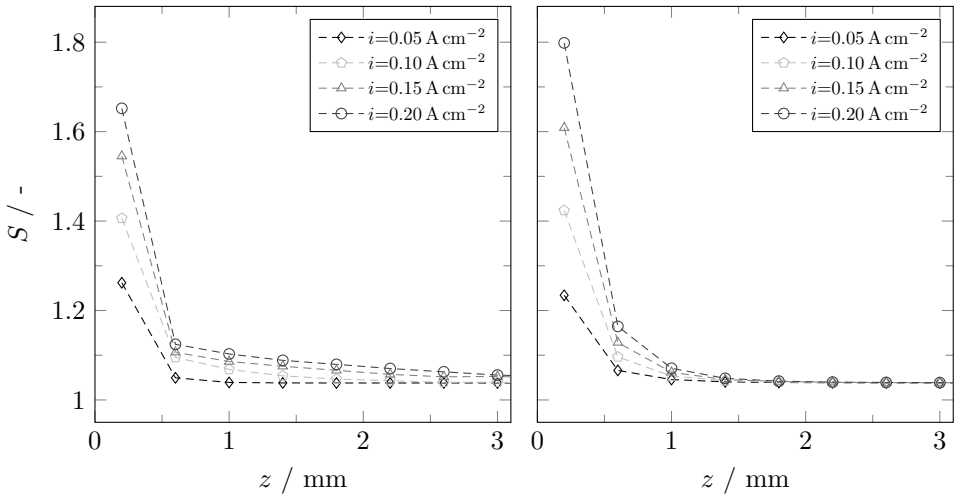


Fig. S.9: Course of local supersaturation within a 3 mm distance to the electrode (z=0) in the (a) A_E = 13.7 cm^2 and (b) A_E = 138 cm^2 electrolyzer at i=0.05, 0.1, 0.15, and 0.2 A cm^{-2} and ζ_{h_E}=0.5.

References

[1] Vanýsek, P.: Ionic conductivity and diffusion at infinite dilution. In: Haynes, W.M. (ed.) CRC Handbook of Chemistry and Physics, 97 edn., pp. 5–75577. CRC Press, Boca Raton, FL, USA (2016)

[2] Mills, R.: Self-diffusion in normal and heavy water in the range 1–45°. The Journal of Physical Chemistry **77**(5), 685–688 (1973) https://doi.org/10.1021/j100624a025

[3] Stewart, P.S.: Diffusion in biofilms. Journal of Bacteriology **185**(5), 1485–1491 (2003) https://doi.org/10.1128/JB.185.5.1485-1491.2003

[4] Cussler, E.L.: Diffusion: Mass Transfer in Fluid Systems. Cambridge University Press, Cambridge, UK (1984)

[5] Kim, H.: Diffusion studies of the systems water–succinic acid–urea and water–succinic acid at 25 °c: The effect of complex formation on the diffusion coefficients of the ternary system. Journal of Solution Chemistry **3**(4), 271–287 (1974) https://doi.org/10.1007/BF00648226